ACS APPLIED MATERIALS & INTERFACES

Research Article

www.acsami.org

Preparation of Superparamagnetic Fe_3O_4@Alginate/Chitosan Nanospheres for *Candida rugosa lipase* Immobilization and Utilization of Layer-by-Layer Assembly to Enhance the Stability of Immobilized Lipase

Xiao Liu, Xia Chen, Yanfeng Li,* Xinyu Wang, Xiaomeng Peng, and Weiwei Zhu

State Key Laboratory of Applied Organic Chemistry, Key Laboratory of Nonferrous Metal Chemistry and Resources Utilization of Gansu Province, College of Chemistry and Chemical Engineering, Institute of Biochemical Engineering & Environmental Technology, Lanzhou University, Lanzhou 730000, China

Supporting Information

ABSTRACT: Superparamagnetic alginate nanospheres with diameter of 50 nm were prepared by self-assembly of alginate in the Ca^{2+} solution; and then superparamagnetic alginate/chitosan nanospheres, which have positive charge and could adsorb lipase directly, were obtained with a following assembly of chitosan based on the electrostatic interaction between alginate and chitosan. Subsequently, oxidic poly (ethylene glycol) was used to functionalize the magnetic alginate/chitosan nanospheres. Thus, the magnetic nanospheres with aldehyde groups and a brushlike structure were formed. With various characterizations, it was verified that the magnetic alginate/chitosan nanospheres held small diameters (around 60 nm) and displayed superparamagnetism with high saturation magnetization. The *Candida rugosa lipase* (CRL), meanwhile, was immobilized onto the magnetic alginate/chitosan nanospheres by electrostatic adsorption and covalent bonding, respectively. Afterward, a layer-by-layer (LBL) assembly process was utilized to coat the immobilized CRL (ICRL) with covering layers made up of alginate and chitosan. After studying the properties of ICRL such as activity, kinetic behaviors, stability and reusability, it was proved that the ICRL prepared with two methods displayed more excellent properties than that prepared with electrostatic adsorption only. Additionally, coating ICRL with covering layers showed good effect on improving the stability of ICRL.

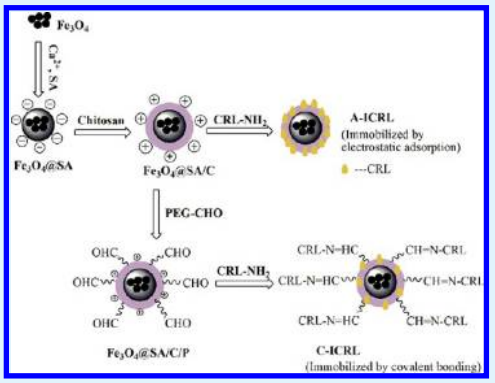

KEYWORDS: *superparamagnetic nanospheres, immobilization, Candida rugosa lipase, layer-by-layer assembly*

1. INTRODUCTION

Enzyme, as is well-known, is superior over chemical catalyst because of its high effectiveness, high specificity, and mild reaction conditions.[1] Lipase (triacylglycerol ester hydrolases, EC 3.1.1.3) is a kind of ubiquitous enzymes with various biological activities, including enantioselective hydrolysis and esterification, chiral resolution, synthesis of enantioenriched monomers, and macromolecules for polymerization, and other enzymatic reactions.[2−4] *Candida rugosa* lipase (CRL), among the lipases from various sources, received much attention due to its high activity and broad specificity. However, the industrial applications of enzyme exist numerous problems such as high operation cost, low stability, difficult recycling and reusing.[5] Compared with free enzyme, immobilized enzyme shows lots of advantages, including catalytic stability, feasible continuous operations, easy recycling, significant reduction of costs, and so on.[6,7]

Recently, various kinds of materials have been used as immobilization supports, such as inorganic materials,[8] synthetic polymers,[9,10] natural polymer,[11] nanoparticles,[12,13] and others. Among different kinds of immobilization supports, magnetic nanoparticles were investigated extensively due to the following advantages:[1] (1) high specific area to favor the binding capacity; (2) low transfer resistance to solve diffusion problem; (3) easily recovery from the reaction system and low operational cost. In addition to immobilization materials, the immobilization methods also have important effect on the activity of immobilized enzyme.[4] There are several commonly used methods, for example, covalent binding,[14] entrapment,[15] adsorption,[16] etc. However, it has been proved that immobilization with two or more methods would greatly increase the loading amount of enzyme and improve the stability of enzyme.[17] Thus, the support with both of positive charge and active groups (such as epoxy group, aldehyde group, etc.) would be a kind of efficient supports.

Alginate and chitosan are two kinds of natural polymers. Alginate is an anionic polysaccharide composed of mannuronic acid and guluronic acid residues, and chitosan is a cationic

Received: June 19, 2012
Accepted: September 17, 2012
Published: September 17, 2012

polysaccharide obtained from partial deacetylation of chitin.[18] On the basis of their electrical properties, they could be used as templates for polyelectrolyte layer-by-layer assembly.[19,20] Chitosan has been used as enzyme immobilization supports for its considerable properties, such as biocompatibility, low cost, various functional group (−OH, $-NH_2$), form versatility (powder, gel beads, fibers, capsules, and membranes) and so on.[21−23] Hung et al[24] prepared a nanofibrous membrane with a fiber diameter of 80−150 nm by an electrospinning process and used the membrane to immobilize *Candida rugosa lipase* with glutaraldehyde as coupling agent, and they achieved a lipase loading of 63.6 mg/g and activity retention of 49.8%. Wang et al.[25] prepared magnetic chitosan nanoparticles and used these nanoparticles to immobilize *glucoamylase* by ionic adsorption, and the protein loading was measured as 12 mg/g support with the immobilization yield of 87%. Kuo et al.[26] prepared magnetic Fe_3O_4-chitosan nanoparticles and used these magnetic chitosan nanoparticles to covalently immobilize the lipase from *Candida rugosa* ultilizing N-(3-dimethylaminopropyl)-N-ethylcarbodiimide (EDC) and N-hydroxysuccinimide (NHS) as coupling agents. The highest activity obtained was 20 U/g Fe_3O_4-chitosan. Wu et al.[27] prepared magnetic chitosan nanoparticles through linking and oxidation in aqueous solution. These nanoparticles were used to immobilize lipase by electrostatic adsorption, and the adsorption loading reached 129 mg/g with the activity retention of 55.6%. Compared with the former reports, lipase immobilization using chitosan nanoparticles displayed excellent performance. Besides, considering the separation and recycling of immobilized enzyme, it is significant to prepare magnetic chitosan spheres with small diameters. Although there have been many literature reports about using chitosan for enzyme immobilization, the magnetic chitosan supports with high loading capacity and low loss of enzyme activity still need to be investigated. PEG is a kind of water-soluble polymer with some outstanding properties such as extensive hydration, good conformational flexibility and considerable chain mobility. In former reports, PEG was grafted as side chains onto other polymer backbone like chitosan[28,29] and poly(L-lysine) .[30] Interestingly, the PEG chains would stretch out into solution to generate a brushlike structure in certain conditions. As a result, PEG would be an excellent bridge to connect supports and enzyme. In addition, utilizing LBL assembly process to form protecting layers has been used in the field of drug encapsulation, and some excellent results has been achieved,[19,31] while there were little relative reports in the field of enzyme immobilization. However, we guess that forming a covering layer on the surface of immobilized enzyme may be an effective strategy to improve its stability.

In this work, efforts were made to prepare superparamagnetic nanoscale supports with high loading capacity and to prepare immobilized lipase with high activity recovery. First, magnetic alginate nanospheres were prepared by self-assembly of alginate in aqueous media containing Ca^{2+}, and then a following layer-by-layer assembly using chitosan was carried out to form magnetic alginate/chitosan nanospheres, which could adsorb lipase directly. These magnetic alginate/chitosan nonaspheres were then functionalized by oxide PEG to obtain the immobilization support with a brush-like structure. Subsequently, *Candida rugosa* lipase (CRL) was immobilized onto different supports by electrostatic adsorption and covalent bonding, respectively. In order to improve the stability of ICRL, a layer-by-layer assembly process was utilized to coat the ICRL with covering layers. At last, the properties of ICRL were investigated including activity, kinetic behaviors, stability, and reusability.

2. MATERIALS AND METHODS

2.1. Materials. Sodium alginate (SA) and chitosan was provided by Tianjing Guangfu Fine Chemical Industry Research Institute (China); *Candida rugosa* Lipase (CRL, Type VII, 1180 units/mg solid) and bovine serum albumin (BSA) were purchased from Sigma Chemical Co.; other chemicals and solvents were all of analytical grade and obtained from Tianjing Chemical Reagent Company (China).

2.2. Preparation of Superparamagnetic Fe_3O_4@SA/Chitosan nanospheres. *2.2.1. Preparation of Fe_3O_4 Nanoparticles.* Fe_3O_4 nanoparticles were prepared by a chemical coprecipitation method described previously[32] with some modifications. Thirty-five milliliters of 1 mol/L $FeCl_2$ and 1.5 mol/L $FeCl_3$ solution were added into a three-necked flask to make the molar ratio of Fe^{2+} and Fe^{3+} maintaining 1:1.5, and the mixture was stirred under nitrogen atmospheres. As the mixture was heated to 60 °C, ammonia (25% w/w) was added to regulate the pH value of the reaction system to 10−11, and the solution became dark after base addition. The solution was then maintained at 80 °C for 1 h with vigorous stirring. After the solution cooled, the precipitates were isolated from reaction system and washed several times with distilled water until the solution became neutral. Finally, the resulting magnetic nanoparticles were obtained after being dried at room temperature under a vacuum.

2.2.2. Preparation of superparamagnetic alginate nanospheres. To prepare superparamagnetic alginate nanospheres, we dispersed 0.24 g of Fe_3O_4 in a flask containing a mixture solution consisting of 20 mL of ethanol and 10 mL of distilled water, and then 40 mL of SA solution (2%) was dropped into the flask. After this, the mixture was vibrated with ultrasonic and stirred vigorously by a mechanical agitator simultaneously under room temperature for 0.5 h. Then, 128 mL of cross-linker, 0.01 M $Ca(OH)_2$ solution, was added into the mixture dropwise. After being stirred sequentially for 1 h, 16 mL of 0.12 M $NaHCO_3$ solution was added into the mixture and stirred for an additional 5 h at room temperature. When reaction completed, the products were separated by permanent magnet and washed thoroughly with ethanol and distilled water. Finally, superparamagnetic sodium alginate nanospheres were obtained after dried at room temperature under vacuum for 12 h, marked as Fe_3O_4@SA.

2.2.3. Preparation and Functionalization of Superparamagnetic Fe_3O_4@SA/Chitosan Nanospheres. On the basis of electrostatic interaction, Fe_3O_4@SA/Chitosan nanospheres were prepared via a self-assembly technique. Two grams of chitosan was dissolved in 200 mL of sodium acetate/acetic acid buffer solution (pH 4.2), and then 2 g of Fe_3O_4@SA nanosphere was added. After being stirred for 30 min at room temperature, the products were separated by permanent magnet and washed thoroughly with ethanol and distilled water until neutral. Finally, the product was dried at room temperature under vacuum for 12 h. Thus, superparamagnetic nanospheres with positive charges were achieved and marked as Fe_3O_4@SA/C.

Herein, PEG-aldehyde (PEG-CHO) was prepared by the oxidation of terminal hydroxyl of PEG according to a former report.[29] 2 g of PEG was dissolved in a DMSO/chloroform mixture under the nitrogen environment. Then 0.2 mL of acetic anhydride was added, and the mixture was stirred for 9 h at room temperature. After that, the white precipitate was obtained by precipitating the mixture in excess dry cold ethyl ether. The white precipitate was then reprecipitated twice from CH_2Cl_2 with ethyl ether. Finally, the white powder, PEG-CHO, was obtained after being dried in a vacuum overnight at room temperature. The resulting PEG-CHO was used to functionalize magnetic support Fe_3O_4@SA/C as follows: a certain amount of Fe_3O_4@SA/C nanoparticle was dispersed in a mixture of methanol and acetic acid (v/v 1:1), and then a certain amount of PEG-CHO was added, making the concentration of PEG-CHO varying from 3% to 30% (m/v). After the mixture stirred for 1 h at 30 °C, the pH value of the mixture was adjusted to 6.0−6.5 with a NaOH aqueous solution. With continues stirring for another 2 h at 30 °C, the reaction was

Scheme 1. Preparation of Magnetic Support and Lipase Immobilization

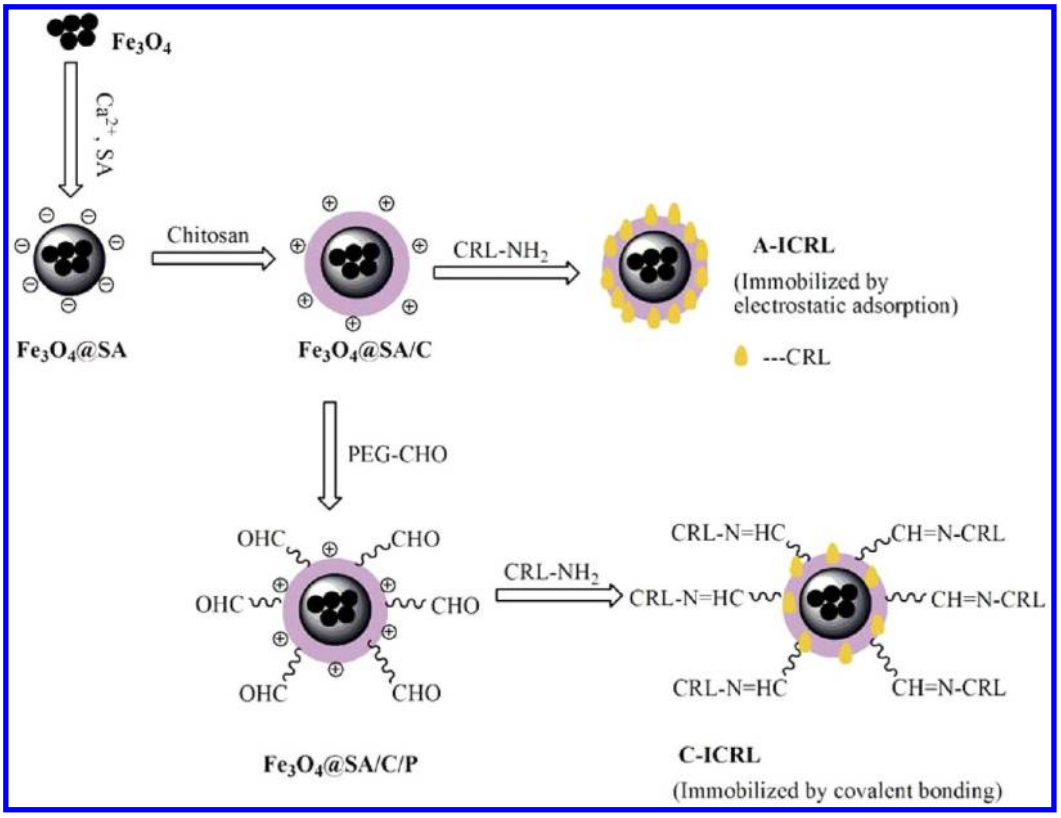

completed and the product was separated by permanent magnet and washed thoroughly with ethanol and distilled water until neutral. At last, the final product was obtained after vacuum drying overnight at room temperature and marked as Fe_3O_4@SA/C/P.

2.3. Characterization of Magnetic Support. The morphologies of Fe_3O_4, Fe_3O_4@SA, and Fe_3O_4@SA/C were observed by transmission electron microscopy (TEM, FEI Tecnai G20). The crystal structure of Fe_3O_4@SA/C was examined by the X-ray diffraction (XRD, Rigaku D/MAX-2400 X-ray diffractometer with Ni-filtered Cu Kα radiation). FT-IR spectra from the KBr pellet with PEG, PEG-CHO, Fe_3O_4, Fe_3O_4@SA, Fe_3O_4@SA/C, and Fe_3O_4@SA/C/P were recorded respectively by a Fourier transform infrared spectrophotometer (Nicole NEXUS 670, USA). Thermogravimetric (TG) analysis of Fe_3O_4@SA and Fe_3O_4@SA/C was observed by a TG-DSC apparatus (NETZSCH STA 449C)) by heating the samples from room temperature to 800 °C under a N_2 atmosphere at a heating rate of 20.0 K/min. The magnetization curves of Fe_3O_4@SA, Fe_3O_4@SA/C and Fe_3O_4@SA/C/P were measured with a vibrating sample magnetometer (LAKESHORE-7304, USA) at room temperature.

2.4. Immobilization of CRL. Herein, both of Fe_3O_4@SA/C and Fe_3O_4@SA/C/P could be used to immobilize lipase. For the two kinds of supports, Fe_3O_4@SA/C has positive charge and could be used to immobilize lipase by electrostatic adsorption, while Fe_3O_4@SA/C/P has both of positive charge and aldehyde group, so lipase could be immobilized on this support by electrostatic adsorption and covalent bonding simultaneously (Scheme 1). Thus, the lipase immobilization was carried out by reaction between lipase solution and magnetic supports directly. Necessary qualities of supports were put into CRL solution (m/v, 1%), then the lipase immobilization was carried out at 30 °C in a shaking-table with rotational speed at 120 rpm for 6 h. After reaction completed, the ICRL was obtained by magnetic separation and washed with distilled water several times to remove the nonimmobilized lipase. The resulted ICRL immobilized by Fe_3O_4@SA/C and Fe_3O_4@SA/C/P were remarked as A-ICRL (immobilized by electrostatic adsorption) and C-ICRL (immobilized by covalent bonding and electrostatic adsorption), respectively. The resulted ICRL was kept at 4 °C prior to use. Especially, the reaction solution and washing solution were collected to assay the amount of residual lipase.

During the immobilization procedure, the amount of lipase added, reaction time and the effect of pH value on the activity of immobilized lipase were investigated, and the relative activity was obtained after incubation under different amount of lipase added (50.0−200 mg/g support), immobilizing time (2−10 h) and pH values (2.0−12.0), respectively.

2.5. Determination of Immobilization Efficiency and Lipase Activity. The immobilization efficiency was expressed by the amounts of enzyme bounded on supports of unite mass, and the amount of enzyme was determined by the Bradford method,[33] using BSA as the standard.

The enzymatic activities of free and immobilized lipase were measured by the titration of the fatty acid which comes from the hydrolysis of olive oil[34] and reverse titration was adopted. One unit of lipase activity (U) is defined as the amount of enzyme needed to hydrolyze olive oil liberating 1.0 μmol of fatty acid per min in the assay condition.

The efficiency of immobilization was evaluated in terms of activity yields and immobilization yield as follows

$$\text{activity yield (\%)} = \frac{C}{A}100\%$$

$$\text{immobilization yield (\%)} = \frac{A-B}{A}100\%$$

Where A is the activity of lipase added in the initial immobilization solution, B is the total activity of the residual lipase in the immobilization and washing solution after the immobilization procedure, and C is the activity of the immobilized lipase, respectively.

The relative activity (%) is the ratio between the activity of every sample and the maximum activity of the sample.

All data used in these formulas are the average of triplicate of experiments.

2.6. Layer-by-Layer Assembly of Chitosan and Alginate for Coating on ICRL. The chitosan and alginate solutions used for

Scheme 2. Layer-by-Layer Assembly of Chitosan and Alginate Covering Layers on A(C)-ICRL

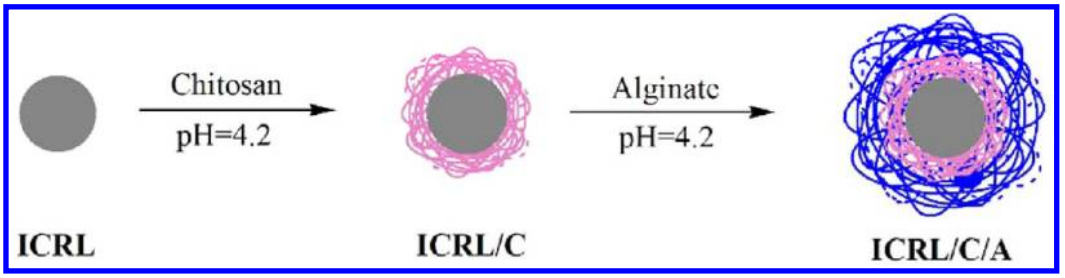

coating on ICRL were prepared at a concentration of 10 mg/mL in sodium acetate/acetic acid buffer solution (pH 4.2). One gram of A(C)-ICRL was dispersed in 50 mL of chitosan solution and the adsorption was carried out at 25 °C in a shaking-table with rotational speed at 130 rpm for 30 min. Then the product was separated with permanent magnet and rinsed repeatedly with a physiological solution. After air-dried at room temperature, the ICRL coated with chitosan (ICRL/C) was achieved. Subsequently, ICRL/C was incubated in an alginate solution and the similar adsorption process was repeated, after which the ICRL coated by two layers was achieved and marked as ICRL/CA. Scheme 2 shows the LBL assembly process. Thus, we prepared two kinds of ICRL without covering layers and four kinds of ICRL coated with covering layers. Herein, ζ-potentials of different ICRL were measured. Subsequently, the stabilities of the six kinds of ICRL in different buffer were assayed: the ICRL were placed in different buffer solutions (pH 3.0, pH 7.0, and pH 12.0) at room temperature, and then the amount of lipase falling off the supports after different time intervals was measured.

2.7. Properties of ICRL. *2.7.1. Effect of pH Value and Temperature on the Enzymatic Activity of FCRL and ICRL.* The effect of pH value on the enzymatic activity of FCRL and the six kinds of ICRL were investigated by hydrolysis of olive oil in a water bath at 37 °Cfor 30 min under a variety of pH value (pH 3.0−12.0), and the relative activity was compared (the relative activity of the ICRL with the highest activity among the six kinds of ICRL was defined as 100%). The temperature endurance of FCRL and the six kinds of ICRL were measured with the relative activity obtained in buffer solutions among the temperature range of 20−80 °C and the relative activity of the ICRL with the highest activity among the six kinds of ICRL was defined as 100% as well

2.7.2. Kinetics of FCRL and ICRL. The Michaelis constant (K_m) and the maximum reaction velocity (V_{max}) of FCRL and the six kinds of ICRL were determined by measuring initial rates of the reaction in phosphate buffer (0.1 M, pH 7.0) at 37 °C. Equivalent FCRL or ICRL was added into olive oil emulsification solutions with different concentrations (0.4−2.0 mg/mL), and the initial activities were determined. K_m and V_{max} values were calculated from initial reaction rate using the Lineweaver−Burk plots with the Michaelis−Menten kinetic equations.

2.7.3. Reusability of ICRL. To assay the reusability of the ICRL, we recovered the ICRL with magnetic separation and washed it with phosphate buffer (0.1 M pH 7.0) after one catalysis run (37 °C, 30 min), and then it was reintroduced into a fresh olive oil solution for catalysis once again. Finally, the activities of the subsequent enzymatic reaction were compared with that of the first run of the ICRL (relative activity defined as 100%).

3. RESULTS AND DISCUSSION

3.1. Preparation and Characterization of Magnetic Nanospheres. *3.1.1. Preparation and Activation of Magnetic Supports.* In this study, two kinds of magnetic supports were prepared and CRL was immobilized onto these supports with different methods, as described in Scheme 1. First, magnetic sodium alginate nanospheres were prepared by an assembly method using Ca^{2+} as the cross-linker, and the ζ-potential of Fe_3O_4@SA was measured as −28.7 mV at pH 4.2. After this, a layer of chitosan was coated on magnetic alginate nanospheres based on electrostatic adsorption (pH 4.2), and then magnetic nanospheres Fe_3O_4@SA/C with a ζ-potential of 34.6 mV (pH 3.0) were obtained, while the ζ-potential of CRL was −2.64 mV at pH 3.0. Thus, Fe_3O_4@SA/C could be used to adsorb CRL directly. Besides, chitosan on the surface of Fe_3O_4@SA/C microspheres has amino groups which could react with aldehyde groups, so Fe_3O_4@SA/C was functionalized by oxide PEG subsequently. Thus, a kind of supports with brushlike structure was achieved. Then, it was used to immobilize CRL by covalent bonding between aldehyde groups and amino groups, as well as electrostatic adsorption. By now, two kinds of ICRL, the A-ICRL prepared only by electrostatic adsorption and the C-ICRL prepared by both of electrostatic adsorption and covalent bonding, were obtained finally.

3.1.2. Characterization of Magnetic Nanospheres. The TEM images of Fe_3O_4 nanoparticles, Fe_3O_4@SA nanospheres, and Fe_3O_4@SA/C nanospheres are given in Figure 1. As shown

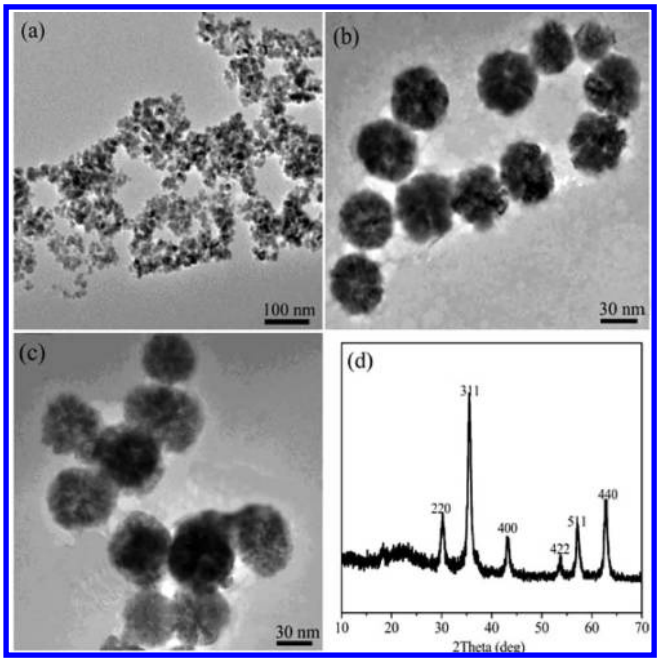

Figure 1. TEM micrographs of (a) Fe_3O_4, (b) Fe_3O_4@SA, (c) Fe_3O_4@SA/C, and (d) XRD of Fe_3O_4@SA/C.

in Figure.1a, the average diameter of Fe_3O_4 nanoparticles we obtained was about 10 nm. Especially, the dispersibility of Fe_3O_4 nanoparticles is terrible because of the interface effects of nanoparticles and the profusive hydroxyl on the surface of nanoparticles. Compared to Figure 1a, the nanospheres in images b and c in Figure 1 not only had larger diameters than Fe_3O_4 nanoparticles but also displayed preferable spherical

shape and uniform size distributions. Relative to the nanospheres with diameters about 50 nm in Figure 1b, the diameters of nanospheres in Figure 1c increased to 60 nm and there was an obvious irregular gray edge. In terms of the morphology mutation given in Figure 1, we can suppose that the preparation of magnetic supports was successful. Besides, the crystal structure of Fe_3O_4@SA/C was characterized as shown in Figure 1d. The indices (220), (311), (400), (422), (511), (440) appeared in this figure could be well-indexed to the inverse cubic spinel structure of Fe_3O_4 (JCPDS card no. 85−1436). This reveals that the modification of magnetic nanospheres did not lead to their crystal phase change .

Figure 2A shows the FT-IR spectra of PEG and PEG-CHO. Compared with Figure 2Aa, there was a new peak that appeared

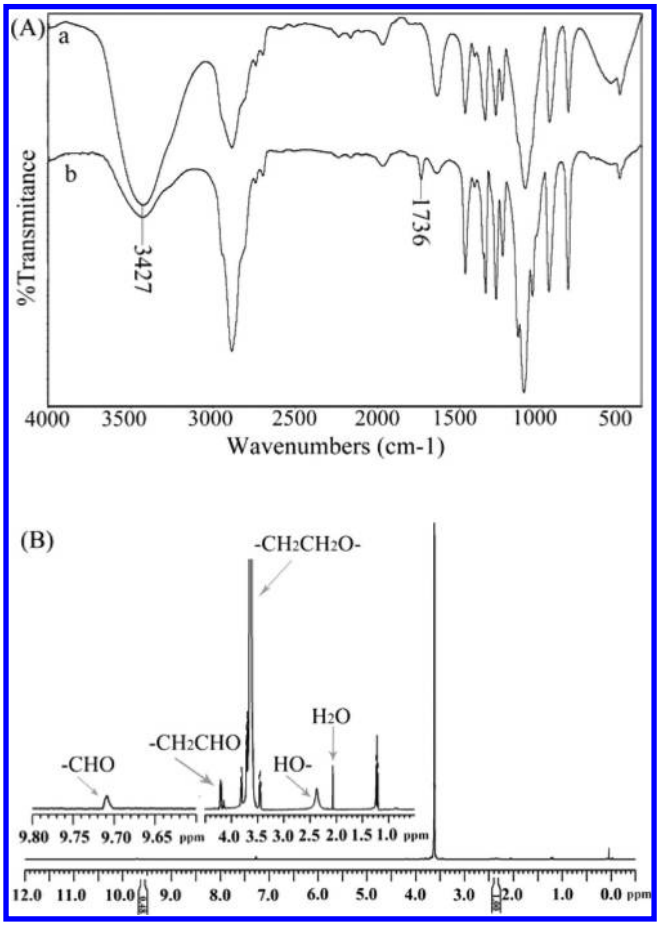

Figure 2. (A) FT-IR spectra of (a) PEG, (b) PEG-CHO, and (B) ^{1}H NMR spectra of PEG-CHO.

at 1736 cm^{-1} in Figure 2Ab, which was due to υ −CHO of PEG-CHO. Additionally, the intensity of hydroxyl vibration peaks of (3427 cm^{-1}) in Figure 2Ab became weaker than that in Figure 2Aa. As a result, the PEG has been oxidized to PEG-CHO. For further investigate the amount of PEG oxidated, the ^{1}H NMR spectra of PEG-CHO are given in Figure 2B. The chemical shifts at 9.78 (−CHO) and 4.20 ppm ($-CH_2CHO$) improved the successful oxidation of PEG, whereas the chemical shifts at 2.31 (−OH) indicated that there were still some hydroxyl groups unoxidized. On the basis of the integral area of the characteristic peaks at 9.78 ppm (−CHO) and 2.31 ppm (−OH), the oxidic proportion of hydroxyl groups could be calculated. When the integral of −OH is marked as 1.00, the integral of −CHO is 0.48. Thus the actual proportion of the hydroxyl groups oxidated is about 32%.

As shown in Figure 3, the characteristic absorption peak of Fe−O bonds in Fe_3O_4 could be found at 560 cm^{-1} clearly in

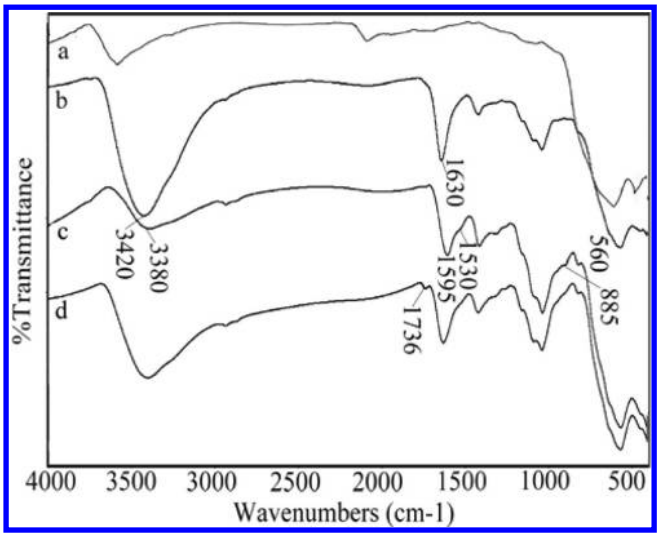

Figure 3. FT-IR spectra of (a) Fe_3O_4, (b) Fe_3O_4@SA, (c) Fe_3O_4@SA/C, and (d) Fe_3O_4@SA/C/P.

Figure 3a and it also could be found in other three spectra. In Figure 3b, the adsorption peaks appeared at 1630 cm^{-1} and 1407 cm^{-1} belonged to the asymmetric and symmetric stretching vibrations of υ-COOH, and the adsorption peak presented at 1026 cm^{-1} should be ascribed to the stretching vibration of alcohol−OH of glucide. Although most structures of chitosan are similar to that of alginate and some peaks would be overlapped mutually, there were still several distinctions in Figure 3c compared with Figure 3b: (1) The original sharp hydroxyl peak (3420 cm^{-1}) became a broader peak and moved to the low frequency, which should be due to the superposition of the stretching vibration of υ-NH_2 on chitosan; (2) The peak at 1630 cm^{-1} in spectra b moved to 1595 cm^{-1} in spectra c and became broader, it was resulted by the overlap between the stretching vibration of υ −COOH and the variable angle vibration of υ -NH_2; (3) Additionally, a new peak appeared at 885 cm^{-1} should be ascribed to the distorted vibration of υ-NH_2. Therefore, chitosan has been coated on the surface of Fe_3O_4@SA successfully. In Figure 3d, the characteristic peal of υ −CHO could be found at 1736 cm^{-1}, which indicated the magnetic nanospheres Fe_3O_4@SA/C has been functionalized with aldehyde group.

The TG analysis of nanospheres Fe_3O_4@SA and Fe_3O_4@SA/C were given in Figure 4. As shown in Figure 4a, a weight loss of 12.64% was observed when temperature rose to 600 °C, indicating that the amount of alginate in Fe_3O_4@SA was 12.64%. Compared with Figure 4a, an additional weight loss about 10.45% was found in Figure 3b when the temperature rose to 760 °C, proving that there were 10.45% of chitosan in Fe_3O_4@SA/C nanospheres. TG analysis also improved that the preparation of magnetic nanospheres was successful.

Figure 5 shows the hysteresis loop of the prepared magnetic spheres. According to Figure 5, the saturation magnetization values of Fe_3O_4@SA, Fe_3O_4@SA/C and Fe_3O_4@SA/C/P were 49.5, 46.1, and 41.0 emu/g, respectively. As a result, these magnetic supports used for CRL immobilization could be

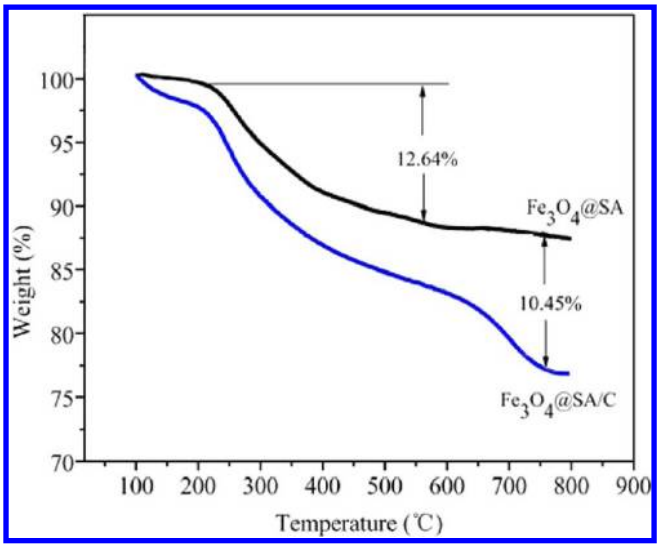

Figure 4. TG curves of Fe_3O_4@SA and Fe_3O_4@SA/C.

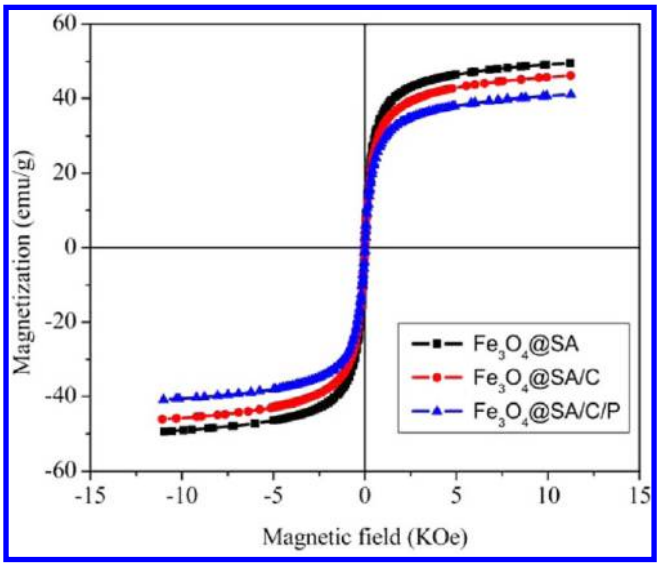

Figure 5. Hysteresis loop of Fe_3O_4@SA, Fe_3O_4@SA/C, and Fe_3O_4@SA/C/P.

separated from the reaction medium rapidly and easily in an external magnetic field. Furthermore, there was no hysteresis in the magnetization with both remanence and coercivity being zero, proving that these magnetic nanospheres are superparamagnetic.[35] Thus, these magnetic supports could respond to an applied magnetic field without any permanent magnetization and redispersed rapidly when the magnetic field disappeared. Compared to the other magnetic nature polymer microspheres prepared in former literature reports,[36,37] the supports we prepared here showed good superparamagnetism and higher saturation magnetization.

3.2. Optimum Amount of PEG-CHO Added. To obtain excellent immobilization efficiency, we investigated the optimum amount of PEG-CHO added by comparing the relative activity of ICRL prepared with various supports functionalized by different amount of PEG-CHO. The functionalized supports were prepared in following conditions: 0.1 g of Fe_3O_4@SA/C nanospheres were dispersed in a mixture of methanol (1 mL) and acetic acid (1 mL), and then a certain amount of PEG-CHO was added, making the concentration of PEG-CHO varying from 3% to 30% (m/v). Then these supports were used to immobilize CRL. The immobilization reaction was taken out at 30 °C for 5 h with the amount of lipase added as 125 mg protein/g support, and the results were showed in Figure 6. According to the data shown in Figure 6,

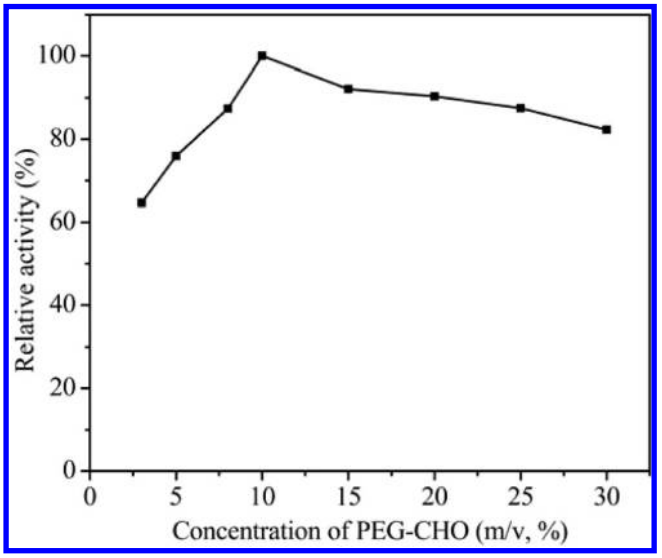

Figure 6. Effect of glutaraldehyde concentrations on immobilization of CRL.

the optimum amount of PEG-CHO added was 10%. When the amount of PEG-CHO added was lower than 10%, the activity of ICRL increased with the increase of PEG-CHO amount, while the reverse results were obtained when the amount of PEG-CHO was higher than 10%. It is considered that the main reason is the overcrowding of functional groups on the surface of magnetic nanparticles, for which the effective covalent bonding between functional groups and lipase was limited.[38,39] Thus, the supports Fe_3O_4@SA/C/P nanospheres used subsequently were activated with PEG-CHO of 20% (2 g PEG-CHO/1 g Fe_3O_4@SA/C).

3.3. Optimum Conditions of CRL Immobilization. After preparing ICRL with different amounts of lipase added, different immobilizing time and different pH values of solutions, the relative activities of these ICRL were compared. And the optimum conditions of immobilizing ICRL were obtained and concluded in Table 1. As shown in Table 1, for Fe@SA/C, the optimum amount of lipase added is 100 mg/g support and the optimum pH is 3, while the optimum amount of Fe@SA/C/P reached 150 mg/g support and the optimum pH is 6. Besides, both of the two kinds of ICRL had the highest activity recovery with a reaction time of 5 h. Thus, the ICRL was prepared under theses optimum conditions. According to Table 1, the loading amounts of lipase for Fe@SA/C and Fe@SA/C/P were 92.78 ± 0.32 mg/g support and 139.87 ± 0.41 mg/g support, respectively. For the two kinds of supports, the reaction time were same, but the optimal amounts of lipase added and optimal pH were different. The amount of protein bonded on Fe@SA/C is lower than that bonded on Fe@SA/C/P, indicating that magnetic Fe@SA/C/P support has better loading capacity. According to the immobilization process (Scheme 1), we can consider that CRL was immobilized on Fe@SA/C support only by electrostatic adsorption. Although CRL immobilized on Fe@SA/C/P could be divided as two parts: on the one hand, CRL was immobilized on supports by

Table 1. Optimal Conditions of Immobilizing Lipase

support	lipase amount added (mg/g)	time (h)	pH	protein bound (mg/g support)	immobilization yield (%)	activity recovery (%)
Fe@SA/C	100	5	3	92.78 ± 0.32	92.78 ± 0.32	62.15 ± 1.34
Fe@SA/C/P	150	5	6	139.87 ± 0.41	93.24 ± 0.37	71.42 ± 1.28

electrostatic adsorption due to the charge performance of chitosan; on the other hand, CRL was immobilized by covalently bonding. Hence, C-ICRL was prepared by two immobilization methods together. However, the covalent bond imines formed between Fe@SA/C/P and lipase is not stable in strong acidic solutions, so the optimal immobilization pH of Fe@SA/C/P moved to pH 6. Thus, it is logical that Fe@SA/C/P nanospheres had better loading capacity than Fe@SA/C. In addition to high loading capacity, the support Fe@SA/C/P also showed higher activity recovery (71.42% ± 1.28%) than Fe@SA/C (62.15% ± 1.34%). The reason may be due to the functionalization of Fe@SA/C with PEG-CHO, which had a long polymer chain and formed a brushlike structure on the surface of Fe@SA/C nanospheres. Thus, the protein bonded onto magnetic support Fe@SA/C/P by PEG-CHO would maintain its original configuration better, and accordingly the CRL immobilized on Fe@SA/C/P had a better activity recovery.

Several literature reports have studied the supports prepared by chitosan for lipase immobilization. In a former literature, magnetic chitosan nanoparticles were prepared and used to immobilize *glucoamylase* by ionic adsorption, and the protein loading was measured as 12 mg/g support with the immobilization yield of 87%.[25] Mendes et al.[40] prepared chitosan-based matrices to immobilize *Thermomyces lanuginosus lipase*, and the maximum loading of protein was 17.5 mg/g gel. Wu et al.[41] prepared chitosan nanoparticles with different methods and immobilized *Cadida rugose lipase* on these nanaparticles. For one support, the lipase adsorption capacity reached 156 mg/g support, and for the other, the lipase adsorption capacity reached 118 mg/g support. For the immobilization studies reported in literatures were investigated in different conditions, it is difficult to compare the immobilization results. Anyway, the results obtained in our study seemed to be quite promising.

3.4. Stabilities of ICRL Coated and Noncoated with Covering Layers in Different Buffers. LBL process had been used to improve the stability of drug molecular embedded in microcapsules[19] and showed significant effect. In this study, chitosan with positive charge and alginate with negative charge were used to form a protective layer on the surface of ICRL, and their ζ-potentials were measured. AS shown in Figure 7, the alternating ζ-potentials observed with each coating step suggested that multilayers were coated on the surface of ICRL with the main driving force of electrostatic adsorption. Additionally, the stabilities of ICRL with or without covering layers in different buffer solutions were compared (Table 2). According to the data in Table 2, several results could be obtained: (1) incubated time: For all kinds of ICRL, the amount of deciduous protein increased with the prolonged incubated time in different buffer solution; (2) pH value: For the ICRL prepared with electrostatic adsorption, the amount of deciduous protein increased with the increase of pH value of the buffer solution, because the electrostatic interaction would be weakened with the increase of pH value. For the ICRL prepared with two immobilization methods, the amounts of deciduous protein in solution of pH 3 and solution of pH 12

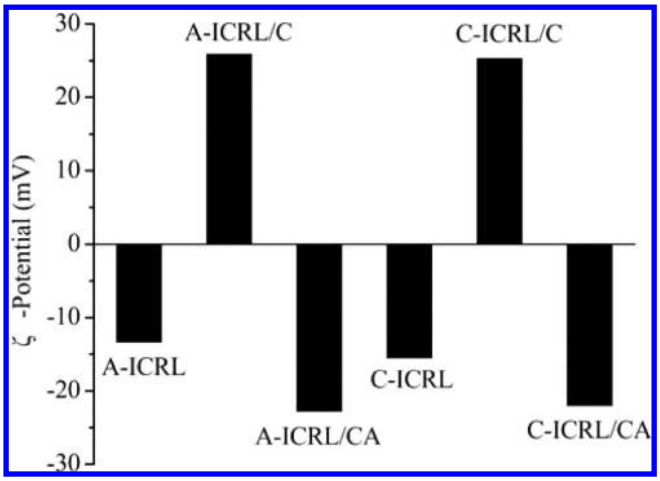

Figure 7. ζ-potential of different ICRL.

Table 2. Stability of ICRL in Different Buffer Solutions

		amount of deciduous protein (%)				
ICRL	pH	2 days	7 days	11 days	30 days	60 days
A-ICRL	3	4.76	5.09	6.25	8.04	9.98
	7	6.84	9.65	9.89	12.8	17.98
	12	28.32	37.26	46.02	60.56	81.34
A-ICRL/C	3	4.49	4.66	5.24	6.85	8.79
	7	6.27	9.49	10.30	11.64	17.88
	12	23.56	31.46	42.85	58.32	80.65
A-ICRL/CA	3	2.17	3.86	4.67	5.39	6.08
	7	5.04	8.16	8.80	10.41	16.13
	12	16.02	24.35	31.79	48.53	75.28
C-ICRL	3	6.93	9.55	14.05	20.36	27.93
	7	3.72	5.51	7.39	7.62	13.12
	12	10.83	14.25	17.36	22.45	29.22
C-ICRL/C	3	5.28	7.54	12.85	18.92	26.64
	7	3.01	5.16	6.99	7.72	12.66
	12	9.65	12.54	14.82	20.29	28.32
C-ICRL/CA	3	4.36	5.28	9.33	13.62	22.17
	7	2.84	4.27	5.25	5.81	8.29
	12	6.03	9.46	12.53	18.69	25.82

are higher than that in neutral solution, as the covalent bond imines are unstable in acidic solution, whereas the electrostatic interaction would be destroyed greatly in basic solution. (3) covering layers: In comparison, the amount of deciduous protein of ICRL without covering layers is obviously higher than that of ICRL with covering layers; (4) the number of covering layers: The amount of deciduous protein of ICRL with one covering layer is higher than that of ICRL with two covering layers, and it means that the covering layers played an important part in improving the stability of ICRL. (5) immobilization methods: In addition to the solution of pH 3, the amount of deciduous protein of the ICRL immobilized with electrostatic adsorption method is distinctly higher than that of the ICRL immobilized with two methods. For A-ICRL, the main immobilization method is electrostatic adsorption, which is highly dependent on the pH value. However, for C-ICRL, the

dx.doi.org/10.1021/am301104c | ACS Appl. Mater. Interfaces 2012, 4, 5169−5178

introduction of covalent bonding improved the stability of ICRL greatly. Thus, the combination of two immobilization methods not only increased the lipase loading amount but also improved the stability of ICRL. On the basis of these results, we can find that the LBL assembly method was an effective procedure to improve the stability of ICRL.

3.5. Optimal conditions of enzymatic activity. *3.5.1. Effect of pH Value and Temperature on the Enzymatic Activity of ICRL.* The effect of pH value on the activities of ICRL was given in Figure 8. It is discovered that the optimal

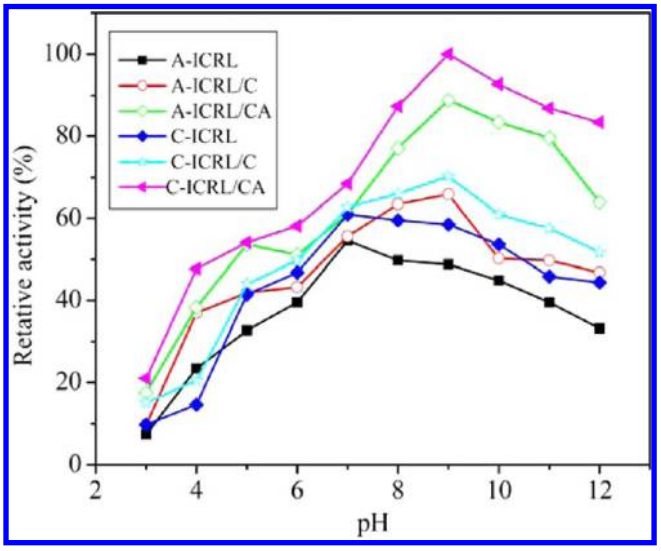

Figure 8. Effect of pH value on the activities of ICRL.

pH value of both A-ICRL and C-ICRL is 7, whereas that of A-ICRL/C, A-ICRL/CA, C-ICRL/C, and C-ICRL/CA shifted to pH 9. In addition, compared to the pH endurance of FCRL (see Figure 1S in the Supporting Information), all the ICRL showed excellent adaptability in a wide pH range especially in the alkaline range. Figure 9 shows the effect of temperature on the activities of ICRL. As shown in Figure 9, the optimal enzymatic temperature of all the ICRL was 50 °C and they played excellent activities when temperature at 40−60 °C.

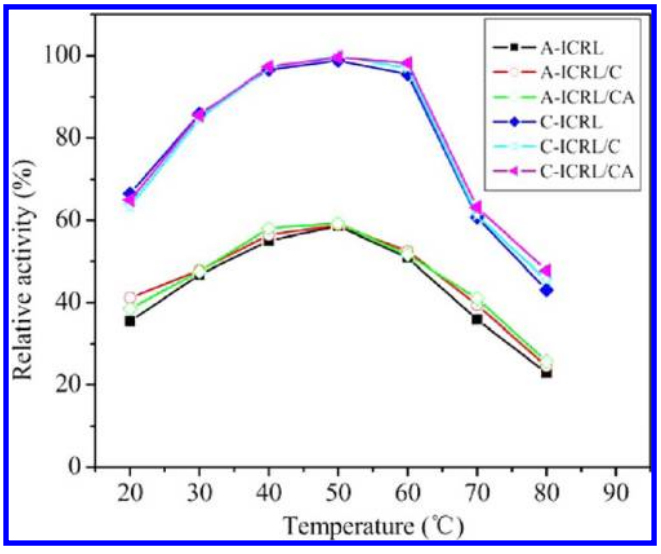

Figure 9. Effect of temperature on the activities of ICRL.

However, the optimal temperature of FCRL was 30−40 °C (see Figure 2S in the Supporting Information). With the changes of pH value or temperature, the A-ICRL (including A-ICRL/C and A-ICRL/C/A) immobilized on Fe_3O_4@SA/C showed significant lower activity than the C-ICRL (including C-ICRL/C and C-ICRL/C/A) immobilized on Fe_3O_4@SA/C/P, indicating that the immobilization method played an important part on the endurance and applicability of immobilized lipase. And the similar result has been reported by other literature.[42] This excellent performance of C-ICRL could be due to the formation of covalent bonds between enzyme and supports, which enhanced the enzyme rigidity and prevented the conformation transition of the enzyme in terrible conditions.[43] In addition, there were obvious activity differences between the ICRL with covering layers and ICRL without covering layers in different pH conditions, and the differences became larger with the increase of pH value. It was proved once again that protecting ICRL with a layer-by-layer process is an effective strategy.

3.5.2. Kinetics of FCRL and ICRL. Kinetics behavior of FCRL and the six kinds of ICRL were investigated by using olive oil with different initial concentrations (0.4−2.0 mg/mL) as the substrates, and the Lineweaver−Burk plots are shown in Figure 10. From the Lineweaver−Burk plots, it could be calculated

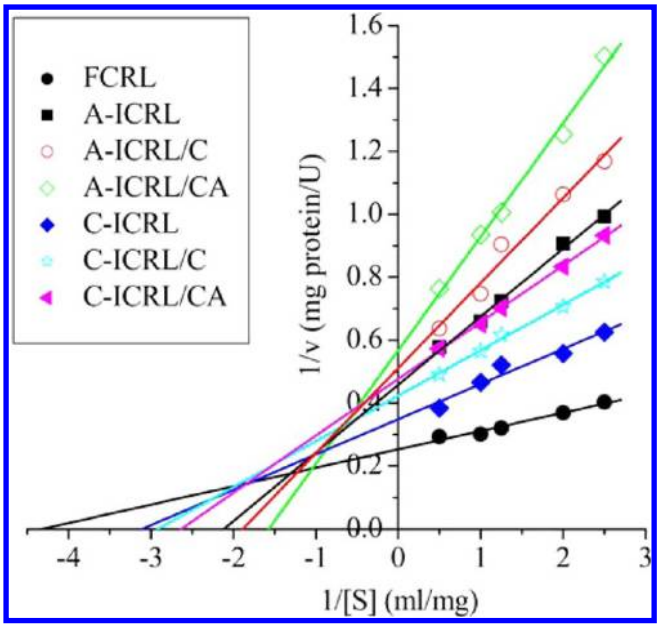

Figure 10. Lineweaver−Burk plots of FCRL and ICRL.

that the K_m value of FICRL was 0.24 mg/mL, whereas that of A-ICRL and C-ICRL were 0.45 and 0.31 mg/mL, respectively. Additionally, the V_{max} value of FCRL (3.99 U/mg lipase) was found to be higher than that of the A-ICRL (2.44 U/mg lipase) and C-ICRL (2.85 U/mg lipase). At first, comparing the kinetic constants of FCRL and ICRL, the increase in K_m and decrease in V_{max} of the six kinds of ICRL indicated that the immobilized lipase has a lower affinity for its substrate than that of free lipase, which may be due to the steric hindrance of the active site caused by supports, the loss of enzyme flexibility necessary for substrate binding, or diffusional resistance to solute transport around the particles.[44] Second, the K_m of A-ICRL was higher than that of C-ICRL and the V_{max} of A-ICRL was lower than that of C-ICRL, and these results also could be

explained by the long flexible chain structure of PEG-CHO as described previously. Third, the order of K_m of ICRL was obtained as follows: A-ICRL < A-ICRL/C < A-ICRL/CA, C-ICRL < C-ICRL/C < C-ICRL/CA, and V_{max} showed exactly the reverse order. It means that the ICRL with covering layers has a lower affinity for its substrate than that of the ICRL without covering layers, which may be ascribed to the mass transfer limitations imposed by the covering layers. Especially, the mass transfer limitations became more obvious with the increase of coating layers.

3.5.3. Reusability of ICRL. The variations of the activity of the six kinds of ICRL after multiple-reuse were shown in Figure 11. According to Figure 11, it could be observed that all of the

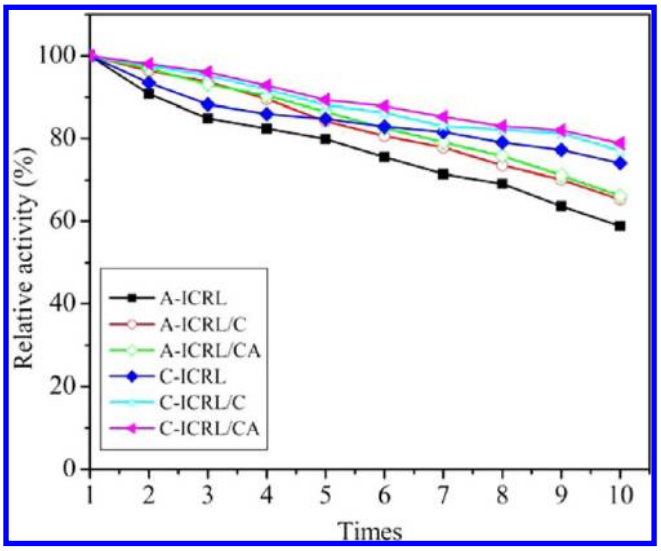

Figure 11. Reusability of ICRL.

ICRL remained good residual activities after the 10th reuse, such as C-ICRL remained 58%, C-ICRL/C remained 65%, C-ICRL/CA remained 66%, A-ICRL remained 74%, A-ICRL/C remained 77%, and A-ICRL/CA remaind 79%. Thus, it could be concluded that the C-ICRL, C-ICRL/C and C-ICRL/CA showed better reusability than A-ICRL, A-ICRL/C, and A-ICRL/CA. Additionally, the ICRL with covering layers showed better reusability than the homologous ICRL without covering layers, although the covering layers could cause certain mass transfer limitations.

4. CONCLUSIONS

In conclusion, superparamagnetic nanospheres were prepared by assembly of alginate and chitosan, and functionalized with oxidic PEG. And then these magnetic supports were used to immobilize CRL with different methods. To improve the stability and applicability of ICRL, a layer-by-layer assembly process was utilized to coat the ICRL with additional covering layers, thus six kinds of ICRL were obtained finally. By means of measuring various properties of ICRL, we find that the immobilization method was important for the stability of ICRL and the method of protecting ICRL with covering layers was an effective strategy. Overall, the ICRL we prepared had high activity recovery and showed excellent properties including pH endurance, temperature endurance, stability, and reusability. All of these remarkable results, together with the good characterization of magnetic nanospheres we prepared, will possibly make them serve as economical and efficient supports for enzyme immobilization

■ ASSOCIATED CONTENT

Supporting Information

The effect of pH value and temperature on the activity of FCRL. This material is available free of charge via the Internet at http://pubs.acs.org/.

■ AUTHOR INFORMATION

Corresponding Author

*Fax: +86 (931) 8912113. E-mail: liyf@lzu.edu.cn.

Notes

The authors declare no competing financial interest.

■ ACKNOWLEDGMENTS

The authors thank the financial supports from the National Natural Science Foundation of China (21074049), the scientific research ability training of under-graduate students majoring in chemistry by the two patters based on the tutorial system and top students (J1103307) and the Opening Foundation of State Key Laboratory of Applied Organic Chemistry (SKLAOC-2009-35)

■ REFERENCES

(1) Hong, J.; Xu, D. M.; Gong, P. J.; Sun, H. W.; Dong, L.; Yao, S. *J. Mol. Catal. B: Enzym.* **2007**, *45*, 84−90.
(2) Gardossi, L.; Bianchi, D.; Klibanov, A. M. *J. Am. Chem. Soc.* **1991**, *113*, 6328−6329.
(3) Jaeger, K.; Reetz, M. *Trends. Biotechnol.* **1998**, *16*, 396−403.
(4) Omprakash, Y.; Toyoko, I. *Biomacromolecules* **2005**, *62*, 809−2814.
(5) Chang, S. W.; Shaw, J. F.; Yang, K. H.; Chang, S. F.; Shieh, C. J. *Bioresour. Technol.* **2008**, *99*, 2800−2805.
(6) Pahujani, S.; Kanwar, S.; Chauhan, G.; Gupta, R. *Bioresour. Technol.* **2008**, *99*, 2566−2570.
(7) Jiang, D. S.; Long, S. Y.; Huang, J.; Xiao, H. Y.; Zhou, J. Y. *Biochem. Eng. J.* **2005**, *25*, 15−23.
(8) Bellezza, F.; Cipiciani, A.; Quotadamo, M. A. *Langmuir* **2005**, *21*, 11099−11104.
(9) Liu, X.; Lei, L.; Li, Y. F.; Zhu, H.; Cui, Y. J.; Hu, H. Y. *Biochem. Eng. J.* **2011**, *56*, 142−149.
(10) Cui, Y. J.; Chen, X.; Li, Y. F.; Liu, X.; Lei, L.; Xuan, S. T. *Appl. Microbiol. Biotechnol.* **2011**, DOI: doi:10.1007/s00253-011-3745-xs.
(11) Natividad, O.; Manuel, P. M.; Maria, C. P.; Maria, D. B. *J. Agric. Food .Chem.* **2009**, *57*, 109−115.
(12) Schatz, A.; Reiser, O.; Stark, W. J. *Chem.—Eur. J.* **2010**, *16*, 8950−8967.
(13) Shylesh, S.; Schunemann, V.; Thiel, W. R. *Angew. Chem., Int. Ed.* **2010**, *49*, 3428−3459.
(14) Hong, J.; Gong, P. J.; Yu, J. H.; Xu, D. M.; Sun, H. W.; Yao, S. *J. Mol. Catal. B: Enzym.* **2006**, *42*, 99−105.
(15) Wang, Y. J.; Caruso, F. *Chem. Mater.* **2005**, *17*, 953−961.
(16) Koutsopoulos, S.; Oost, J.; Norde, W. *Langmuir* **2004**, *20*, 6401−6406.
(17) Pessela, B. C. C.; Mateo, C.; Carrascosa, A. V.; Vian, A.; Garcia, J. L.; Rivas, G.; Alfonso, C.; Guisan, J. M.; Lafuente, R. F. *Biomacromolecules* **2003**, *4*, 107−113.
(18) Jaejoon, H.; Annes, O. G.; Stephane, S.; Monique, L. *J. Agric. Food. Chem.* **2008**, *56*, 2528−2535.
(19) Liu, J. W.; Zhang, Y.; Wang, C. Y.; Xu, R. Z.; Chen, Z. P.; Gu, N. *J. Phys. Chem. C.* **2010**, *114*, 7673−7679.
(20) Xie, H. G.; Zheng, J. N.; Li, X. X.; Liu, X. D.; Zhu, J.; Wang, F.; Xie, W. Y.; Ma, X. J. *Langmuir* **2010**, *26*, 5587−5594.
(21) Silva, J. A.; Macedo, G. P.; Rodrigues, D. S.; Giordano, R. L. C.; Goncalves, L. R. B. *Biochem. Eng. J.* **2012**, *60*, 16−24.

(22) Amorim, R. V. S.; Melo, E. S.; Carneiro-da-Cunha, M. G.; Ledingham, W. M.; Campos-Takaki, G. M. *Bioresour. Technol.* **2003**, *89*, 3.5−39.
(23) Yi, S. Se.; Noh, J. M.; Lee, Y. S. *J. Mol. Catal. B: Enzym.* **2009**, *57*, 123−129.
(24) Huang, X. J.; Ge, D.; Xu, Z. K. 2007. *Eur. Polym. J.* **2007**, *43*, 3710-3718.
(25) Wang, J. Z.; Zhao, G. H.; Li, Y. F.; Liu, X.; Hou, P. P. *Appl. Microbiol. Biotechnol.* **2012**, DOI: 10.1007/s00253-012-3979-2.
(26) Kuo, C. H.; Liu, Y. C.; Chang, C. M. J.; Chen, J. H.; Chang, C.; Shieh, C. J. *Carbohyd. Polym.* **2012**, *87*, 2538−2545.
(27) Wu, Y.; Wang, Y. J.; Luo, G. S.; Dai, Y. Y. *Bioresour. Technol.* **2009**, *100*, 3459−3464.
(28) Ye, Z.; Bo, L.; Natalija, G.; Ricardas, M.; Andra, D.; Per, M. C. J. *J. Colloid .Interface. Sci.* **2007**, *305*, 62−71.
(29) Zheng, J. N.; Xie, H. G.; Yu, W. T.; Liu, X. D.; Xie, W. Y.; Zhu, J.; Ma, X, J. *Langmuir* **2010**, *26*, 17156−17164.
(30) Stephanie, P.; Susan, M.; De, P.; Janos, V.; Nichol, D. S.; Marcus, T. *Langmuir* **2003**, *19*, 9216−9225.
(31) Zhu, H.; Srivastava, R.; Srivastava, R.; McShane, M. J. *Biomacromolecules* **2005**, *6*, 2221−2228.
(32) Massart, R.; Cabuil, V. *J. Chim. Phys. Phys-Chim. Biol.* **1987**, *84*, 967−973.
(33) Bradford, M. M. *Anal. Biochem.* **1976**, *72*, 248−254.
(34) Watanabe, N.; Ota, Y.; Minoda, Y.; Yamada, K. *Agric. Biol. Chem.* **1977**, *41*, 1353−1358.
(35) Mooney, K. E.; Nelson, J. A.; Wagner, M. J. *Chem. Mater.* **2004**, *16*, 3155−3161.
(36) Finotelli, P. V.; Morales, M. A.; Rocha-Leao, M. H.; Baggio-Saitovitch, E. M.; Rossi, A. M. *Mater. Sci. Eng., C* **2004**, *24*, 625−629.
(37) Yoshiyuki, N.; Akiko, Y.; Kana, E.; Yoshiharu, M.; Hidemitsu, F.; Kazuyuki, H. *Polymer* **2004**, *45*, 7129−7136.
(38) Bayramoglu, G.; Kiralp, S.; Yilmaz, M.; Toppare, L.; Arıca, M. Y. *Biochem. Eng J.* **2008**, *38*, 180−188.
(39) Jiang, D. S.; Long, S. Y.; Huang, J.; Xiao, H. Y.; Zhou, J. Y. *Biochem. Eng J.* **2005**, *25*, 15−23.
(40) Mendes, A. A.; Castro, H. F.; Rodrigues, D. S.; Adriano, W. S.; Tardioli, P. W.; Mammarella, E. J.; Giordano, R. C.; Giordano, R. L. C. *J. Ind. Microbiol. Biotechnol.* **2011**, *38*, 1055−1066.
(41) Wu, Y.; Wang, Y. J.; Luo, G. S.; Dai, Y. Y. *Bioresour. Technol.* **2010**, *101*, 841−844.
(42) Bayranglu, G.; Kiralp, S.; Yilmaz, M.; Toppore, L.; Arica, M. Y. *Appl. Microbiol. Biotechnol.* **2012**, DOI: 10.1007/s00253-012-3999-y.
(43) Xi, F. N.; Wu, J..M.; Jia, Z. S.; Lin, X. F. *Process. Biochem.* **2005**, *40*, 2833−2840.
(44) Chang, M. Y.; Juang, R. S. *Enzym. Microb. Technol.* **2005**, *36*, 75−82.